Volume 10, Issue 4, 2020, 5869 - 5874 ISSN 2069-5837

Biointerface Research in Applied Chemistry

www.BiointerfaceResearch.com

https://doi.org/10.33263/BRIAC104.869874

Original Research Article Open Access Journal

Received: 02.04.2020 / Revised: 20.04.2020 / Accepted: 21.04.2020 / Published on-line: 22.04.2020

Design and synthesis of some imidazole derivatives: theoretical evaluation of interaction with a coronavirus (HCoV-NL63)

Figueroa-Valverde Lauro[1, *], Díaz-Cedillo Francisco [2], Rosas-Nexticapa Marcela [3,*], López-Ramos Maria [1], Mateu-Armad Maria Virginia [3], Garcimarrero E. Alejandara [4], Cauich-Carrillo Regina [1]

[1]Laboratory of Pharmaco-Chemistry, Faculty of Chemical Biological Sciences, University Autonomous of Campeche, Av. Agustín Melgar s/n, Col Buenavista C.P. 24039 Campeche, Camp., México

[2]Escuela Nacional de Ciencias Biológicas del Instituto Politécnico Nacional. Prol. Carpio y Plan de Ayala s/n Col. Santo Tomas, México

[3]Facultad de Nutrición, Universidad Veracruzana, Médicos y Odontologos s/n C.P. 91010, Unidad del Bosque Xalapa Veracruz, México

[4]Facultad de Medicina, Universidad Veracruzana, Médicos y Odontologos s/n C.P. 91010, Unidad del Bosque Xalapa Veracruz, México

*corresponding author e-mail address: ***lfiguero@uacam.mx; rosasnm@yahoo.com.mx*** | Scopus ID 55995915500

ABSTRACT

Some compounds have been developed for the treatment of Severe Acute Respiratory Syndrome Coronavirus (SARS-CoV) using different protocols; however, some methods use different reagents which are dangerous and require special conditions. the objective of this investigation was to synthesize some imidazole derivatives from 2-methyl-5-nitroimidazole using some reactions such as etherification, reduction, and a hydroxy-keto derivative formation. In addition, the theoretical activity of imidazole derivatives (compounds **2**, **3** and **5**-**8**) was evaluated in a docking model using hydroxylchloroquine and favipiravir as controls. The results showed that 1) compounds **3** and **5** have a higher affinity by 5ewp protein surface compared with hydroxylchloroquine, favipiravir, **2** and **6**-**8**. In conclusion, compounds **3** and **5** could inhibit the biological activity of coronavirus.

Keywords: *Imidazole; derivative; coronavirus; hydroxylchloroquine; favipiravir.*

1. INTRODUCTION

Severe acute respiratory syndrome (SARS) contributes substantially to incidence and premature mortality worldwide. It is noteworthy that SARS has been associated with a series of coronavirus (SARS-CoV) [1-3].

In the search of some drug for treatment for SARS-CoV several compounds have been developed. For example, the preparation of compound 4-(*Z*-Leu-amido)-6-fluoro-5-oxohexanoic Acid Dimethylamide from 4-Amino-6-fluoro-5-hydroxyhexanoic Acid Dimethylamide [4]. In addition, other study showed the synthesis of (S)-N-benzyl-3-((S)-2-cinnamamido-3-cyclopentyl-propanamido)-2-oxo-4-((S)-2-oxo-pyrrolidin-3-yl)butanamide via oxidation of a α-hydroxyamide derivative with periodinane (Dess-Martin reagent). [5]. Other report indicates the reaction of 2,3-Dioxo-2,3-dihydro-1H-indole-5-carboxylic acid amide with 2-(bromomethyl)naphthalene to form the compound 1-Naphthalen-2-ylmethyl-2,3-dioxo-2,3-dihydro-1H-indole-5-carboxylic acid amide [6]. In addition, other study showed the preparation of compound (*R*)-N-(4-(tert-butyl)phenyl)-N-(2-(tert-butyla-mino)-2-oxo-1-(pyridin-3-yl)ethyl)furan-2-carboxamide from pyridine-3-carboxaldehyde, 4-tert-butylaniline, and furan-2-carboxylic acid [7].

Additionally, a report indicated the synthesis of benzyl-ami- no]carbonyl piperidine *via* reaction of 1-[(R)-1-(1-Naphthyl)ethyl]-4-methoxycarbonylpiperidine with dimethylforma-mide [8]. In addition, a study showed the synthesis of a keto-glutamine analogue from N-Boc-*L*-phenylalanine [9]. All these data have shown the preparation of several compounds with activity on some SARS-CoV strains. However, the protocols use some reagents which are dangerous and require special conditions.

Analyzing these data, the aim of this research research was to synthesize some imidazole derivatives to evaluate their theoretical activity against the coronavirus (HCoV-NL63) in a docking model.

2. MATERIALS AND METHODS

The reagents used in this investigation were acquired from Sigma-Aldrich Co., Ltd. The melting point for compounds was evaluated on an Electrothermal (900 model). Infrared spectra (IR) were evaluated with a Thermo Scientific iSOFT-IR spectrometer.^{1}H and ^{13}C NMR spectra were recorded using a Varian VXR300/5 FT NMR spectrometer at 300 MHz in $CDCl_3$ using TMS as an internal standard. EIMS spectra were obtained with a Finnigan Trace Gas Chromatography Polaris Q-Spectrometer. Elementary analysis data were acquired from a Perkin Elmer Ser. II CHNS/02400 elemental analyzer.

2.1. Etherification reaction.

2-((2-methyl-1H-imidazol-5-yl)oxy)-1-naphthaldehyde (2)

In a round bottom flask (10 ml), 2-methyl-5-nitroimidazole (200 mg, 0.67 mmol), 2-hydroxy-1-naphthaldehyde (110 mg, 0.67 mmol). potassium carbonate anhydrous (0.60 mg, 0.43 mmol) and 5 ml of dimethyl sulfoxide were stirred at room temperature for 72 h. Then, the solvent was evaporated under reduced pressure and following the product was purified via crystallization using the methanol:water (3:1) system; yielding 55% of product; m.p. 140-142 °C; IR (V_{max}, cm^{-1}) 3450, 1722 and 1224: ^{1}H NMR (300 MHz, $CDCl_3$-*d*) δ_H: 2.42 (s, 3H), 6.60 (m, 1H), 7.36-9.40 (m, 6H), 10.70 (s, 1H), 11.32 (broad, 1H) ppm. ^{13}C NMR (300 Hz, $CDCl_3$) δ_C: 13.92, 116.26, 116.85, 119.66, 124.52, 124.90, 126.38, 128.22, 129.62, 133.61, 134.94, 141.52, 151.90, 155.34,

192.90 ppm. EI-MS m/z: 252.08. Anal. Calcd. for $C_{15}H_{12}N_2O_2$: C, 71.42; H, 4.79; N, 11.10; O, 12.68. Found: C, 71.40; H, 4.77.

2.2. Synthesis a keto-hydroxy derivative.

N1-[2-(2-Methyl-3H-imidazol-4-yloxy)-naphthalen-1-ylmethylene]-ethane-1,2-diamine (3)

To a 10 ml bottom flask was added the compound **2** (200, 0.79 mmol), ethylenediamine (60 µl 0.90 mmol), boric acid (60 mg, 0.97 mmol) 5 ml of methanol. The mixture was stirred at room temperature for 72 h. Then, the solvent was evaporated under reduced pressure and following the product was purified via crystallization using the methanol:water (4:1) system; yielding 58% of product; m.p. 188-190 °C; IR (V_{max}, cm^{-1}) 3380, 3450 and 1222: ^{1}H NMR (300 MHz, $CDCl_3$-*d*) δ_H: 2.42 (s, 3H), 3.10-3.80 (m, 4H), 6.44 (m, 1H), 7.01 (broad, 3H), 7.44-8.70 (m, 6H), 9.06 (m, 1H) ppm. ^{13}C NMR (300 Hz, $CDCl_3$) δ_C: 13.92, 40.66, 54.92, 114.56, 115.38, 122.62, 122.66, 124.74, 128.08, 128.80, 129.86, 130.66, 136.60, 141.50, 151.15, 151.90, 162.10 ppm. EI-MS m/z: 294.14. Anal. Calcd. for $C_{17}H_{18}N_4O$: C, 69.37; H, 6.16; N, 19.03; O, 5.44. Found: C, 69.35; H, 6.14.

2.3. Synthesis of a keto-hydroxy derivative.

(R)-4-hydroxy-5-(2-((2-methyl-1H-imidazol-5-yl)oxy)naphtha- len-1-yl)pentan-2-one (5)

To a 10 ml bottom flask was added the compound **2** (200, 0.79 mmol), acetone (5 ml), 5 ml of methanol and *L*-proline (100 mg, 0.87 mmol). The mixture was stirred at reflux for 12 h. Then, the solvent was evaporated under reduced pressure and following the product was purified via crystallization using the methanol:hexane:water (3:1:1) system; yielding 44% of product; m.p. 200-202 °C; IR (V_{max}, cm^{-1}) 3450, 3400, 1712 and 1224: ^{1}H NMR (300 MHz, $CDCl_3$-*d*) δ_H: 2.10 (s, 3H), 2.42 (s, 3H), 2.63-2.76 (m, 2H), 3.00-3.14 (m, 2H), 4.30 (m, 1H), 6.32 (m, 1H), 7.30-7.96 (m, 6H), 8.08 (broad, 2H) ppm. ^{13}C NMR (300 Hz, $CDCl_3$) δ_C: 13.92, 30.42, 37.76, 50.66, 70.10, 110.62, 117.64, 122.80, 127.74, 128.56, 128.82, 129.42, 129.54, 131.02, 141.52, 150.44, 151.92, 153.24, 203.62 ppm. EI-MS m/z: 324.14. Anal. Calcd. for $C_{19}H_{20}N_2O_3$: C, 70.35; H, 6.21; N, 8.64; O, 14.80. Found: C, 70.32; H, 6.20.

2.4. Second etherification reaction.

(R)-2-(4-((1-(2-((2-methyl-1H-imidazol-5-yl)oxy)naphthalen-1-yl)-4-oxopentan-2-yl)- oxy)phenyl)acetonitrile (6)

To a 10 ml bottom flask was added the compound **5** (200, 0.61 mmol), 2-(4-nitrophenyl)acetonitrile (100 mg, 0.61 mmol), potassium carbonate anhydrous (0.60 mg, 0.43 mmol) and 5 ml of dimethyl sulfoxide. The mixture was stirred at room temperature for 48 h. Then, the solvent was evaporated under reduced pressure and following the product was purified via crystallization using the methanol:water (4:1) system; yielding 66% of product; m.p. 178-180 °C; IR (V_{max}, cm^{-1}) 3450, 2240, 1712 and 1222: ^{1}H NMR (300 MHz, $CDCl_3$-*d*) δ_H: 2.12 (s, 3H), 2.42 (s, 3H), 2.66-2.86 (m, 2H), 3.04-3.20 (m, 2H), 3.62 (m, 2H), 4.88 (m, 1H), 6.32 (m, 1H), 6.97-7.28 (m, 4H), 7.36-7.96 (m, 6H), 11.34 (broad, 1H) ppm. ^{13}C NMR (300 Hz, $CDCl_3$) δ_C: 13.92, 23.44, 30.44, 36.84, 49.70, 82.30, 110.62, 117.42, 117.50, 117.52, 122.74, 122.80, 127.20, 127.60, 129.52, 129.74, 130.36, 133.66, 141.50, 147.30, 151.90, 153.62, 159.32, 200.84 ppm. EI-MS m/z: 439.18. Anal. Calcd. for $C_{27}H_{25}N_3O_3$: C, 73.78; H, 5.73; N, 9.56; O, 10.92. Found: C, 73.76; H, 5.70.

2.5. Reduction reaction.

(2R)-1-(2-((2-methyl-1H-imidazol-5-yl)oxy)naphthalen-1-yl)pentane-2,4-diol (7)

To a 10 ml bottom flask was added the compound **6** (200 mg, 0.45 mmol) sodium borohydride (30 mg, 0.79 mmol) and 5 ml of ethanol. The mixture was stirred at room temperature for 72 h. Then, the solvent was evaporated under reduced pressure and following the product was purified via crystallization using the methanol:water (4:1) system; yielding 73% of product; m.p. 138-140 °C; IR (V_{max}, cm^{-1}) 3450, 3400 and 1224: ^{1}H NMR (300 MHz, $CDCl_3$-*d*) δ_H: 1.22 (s, 3H), 1.52-1.56 (m, 2H), 2.42 (s, 3H), 2.88-3.04 (m, 2H), 3.98-4.28 (m, 2H), 5.70 (broad, 3H), 6.32 (m, 1H), 7.26-7.94 (m, 6H) ppm. ^{13}C NMR (300 Hz, $CDCl_3$) δ_C: 13.92, 23.90, 37.30, 49.44, 65.94, 69.82, 110.62, 117.28, 122.80, 127.40, 128.58, 128.80, 128.82, 129.42, 133.20, 141.50, 147.84, 151.90, 153.10 ppm. EI-MS m/z: 326.16. Anal. Calcd. for $C_{19}H_{22}N_2O_3$: C, 69.92; H, 6.79; N, 8.58; O, 14.71. Found: C, 69.90; H, 6.76.

2.6. Third etherification reaction.

2,2'-((((2R)-1-(2-((2-methyl-1H-imidazol-5-yl)oxy)naphthalen-1-yl)pentane-2,4-diyl)- bis(oxy))bis(4,1-phenylene))diacetone- trile (8)

To a 10 ml bottom flask was added the compound **7** (200 mg, 0.61 mmol), 2-(4-nitrophenyl)acetonitrile (100 mg, 0.61 mmol), potassium carbonate anhydrous (0.60 mg, 0.43 mmol) and 5 ml of dimethyl sulfoxide. The mixture was stirred at room temperature for 72 h. Then, the solvent was evaporated under reduced pressure and following the product was purified via crystallization using the methanol:water (4:1) system; yielding 73% of product; m.p. 196-198 °C; IR (V_{max}, cm^{-1}) 3450, 2240 and 1224: ^{1}H NMR (300 MHz, $CDCl_3$-*d*) δ_H: 1.32 (s, 3H), 2.02-2.20 (m, 2H), 2.42 (s, 3H), 3.00-3.14 (m, 2H), 3.62 (m, 4H), 4.50-5.02 (m, 2H), 6.32 (m, 1H), 6.80 -7.20 (m, 8H), 7.30-7.92 (m, 6H), 11.34 (broad, 1H) ppm. ^{13}C NMR (300 Hz, $CDCl_3$) δ_C: 13.92, 21.54, 23.44, 36.74, 47.54, 75.60, 80.22, 110.60, 116.08, 117.12, 117.40, 118.34, 122.74, 122.80, 127.04, 127.22, 129.44, 129.52, 129.74, 130.36, 135.92, 141.50, 146.56, 151.90, 154.42, 1567.26, 158.40 ppm. EI-MS m/z: 556.24. Anal. Calcd. for $C_{35}H_{32}N_4O_3$: C, 75.22; H, 5.79; N, 10.06; O, 8.62. Found: C, 75.20; H, 5.76.

2.7. Pharmacophore evaluation.

The 3D pharmacophore model for the compounds **3** and **4** was determinate using LigandScout 4.08 software [10, 11].

2.8. Theoretical evaluation of the interaction between imidazole derivatives with coronavirus, HCoV-NL63 (3epw protein).

The interaction of imidazole derivatives with 3epw protein [12] was carried out using a DockingServer [13].

3. RESULTS

Various drugs have been prepared for the treatment of SARS-CoV (4-9); however, some of these compounds have different biological activities against the coronavirus (HCoV-NL63). In this way, in this investigation were prepared some imidazole derivatives to evaluate their theoretical activity against coronavirus using 5epw protein [12] as a chemical tool. The first stage was achieved as follows:

3.1. Chemical synthesis.

3.1.1. Etherification reaction.

Several protocols have been used to preparation of ether derivatives using some reagents such as $ZbBr_2$ [14], Bis(cyclooctadiene)nickel [15] ether-imidazolium chlorides [16], lithium binaphtholate [17] and others. In this study, the compound **2** was prepared via displacement of nitro group of compound **1** by hydroxyl group of 2-hydroxy-1-naphthaldehyde in the presence of dimethyl sulfoxide at middle conditions (Figure 1).

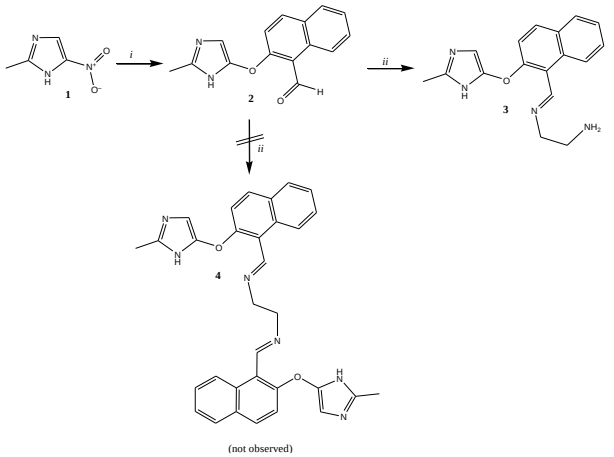

Figure 1. Synthesis of *N*[1]-[2-(2-Methyl-3H-imidazol-4-yloxy)-naphthalen-1-yl-methylene]-ethane-1,2-diamine (**3**). Reaction of 2-methylnitroimidazole with 2-hydroxy-1-naphthaldehyde (*i*) to form 2-((2-methyl-1H-imidazol-5-yl)oxy)-1-naph-thaldehyde (**2**). then, **2** reacted with ethylenediamine (*ii*) to form **3**.

The ^{1}H NMR spectrum of **2** (Figure 1) showed several signals at 2.42 ppm for methyl group bound to imidazole ring; at 6.60 ppm for imidazole ring; at 7.39-9.40 ppm for naphthalene group; at 10.70 ppm for aldehyde group; at 11.32 ppm for amino group. In addition, the ^{13}C NMR spectra display chemical shifts at 13.92 ppm for methyl group bound to imidazole ring; at 116.26, 119.66-134.94 and 155.34 ppm for naphthalene group; at 116.85 and 141.52-151.90 ppm for imidazole ring; at 192.91 ppm for imidazole ring. Additionally, the mass spectrum from **2** showed a molecular ion (m/z) 252.08.

3.1.2. Preparation of an imino derivative.

There are some protocols for the preparation of several imino derivatives; nevertheless, in this investigation, boric acid was used as catalyst, because it is not an expensive reagent and special conditions for its use are not required [18]. The ^{1}H NMR spectrum of **3** (Figure 1) showed several signals at 2.42 ppm for methyl group bound to imidazole ring; at 3.10-3.80 ppm for methylene groups linked to both amino groups; at 6.44 ppm for imidazole ring; at 7.01 ppm for the amino group; at 7.44-8.70 ppm for naphthalene group; at 9.06 ppm for imino group. The ^{13}C NMR spectra display chemical shifts at 13.92 ppm for methyl group bound to imidazole ring; at 40.66-61.30 ppm for methylene linked to both amino groups; at 114.56, 141.50 and 151.90 ppm for imidazole ring; at 115.38-136.60 and 151.15 ppm for naphthalene group; at 162.10 ppm for imino group. Finally, the mass spectrum from **3** showed a molecular ion (m/z) 294.14.

3.1.3. Synthesis a keto-hydroxy derivative.

Several hydroxy-keto derivatives have been prepared using some protocols; however, some methods use reagents that are expensive and require special conditions [19]. In addition, a study showed the preparation of hydroxy-keto derivatives via reaction of ketone and aldehyde groups in the presence of *L*-proline [20].

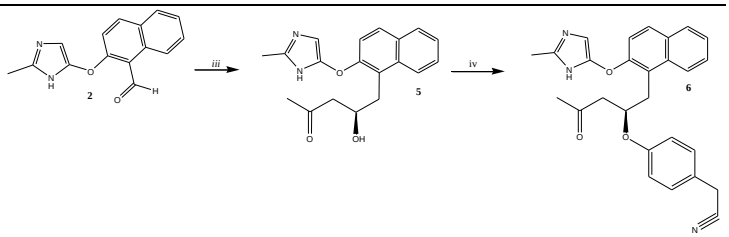

Figure 2. Synthesis of an imidazole-naphtalene acetonitrile (**6**). Reaction of 2-((2-methyl-1H-imidazol-5-yl)oxy)-1-naph-thaldehyde (**2**) with acetone/proline (*iii*) to form a hydroxy-keto derivative (**5**). Then **5** reacted with 2-(4-nitrophenyl)acetonitrile/dimethyl sulfoxide (iv) to form **6**.

Analyzing these data, in this research, a hydroxy-keto derivative (**5**) was synthesized from compound **2**, acetone and *L*-proline (Figure 2). The ^{1}H NMR spectrum of **5** showed several signals at 2.42 ppm for methyl group bound to imidazole ring: at 2.10 ppm for methyl bound to ketone group; at 2.63-2.76 ppm for methylene groups linked to both ketone and hydroxyl groups; at 3.00-3.14 ppm for methylene bound to phenyl group; at 4.30 ppm for methylene bound to hydroxyl group; at 6.32 ppm for imidazole ring; at 7.30-7.96 ppm for naphthalene group; at 8.08 for both amino and hydroxyl groups. The ^{13}C NMR spectra showed chemical shifts at 13.92 ppm for methyl group bound to imidazole ring; at 30.42 ppm for methyl bound to ketone group; at 37.76 for methylene bound to phenyl group; at 50.66 ppm for methylene group linked to both hydroxyl and ketone groups; at 70.10 ppm for methylene bound to hydroxyl group; at 110.62, 141.52 and 151.92 ppm for imidazole ring; at 117.64-131.02, 150.44 and 153.24 ppm for naphthalene group; at 203.62 ppm for ketone group. Additionally, the mass spectrum from **5** showed a molecular ion (m/z) 324.14.

3.1.4. Second etherification.

The imidazol-naphthalen-acetonitrile derivative (**6**) was prepared via reaction of compound **5** with 2-(4-nitrophenyl)acetonitrile in the presence of dimethyl sulfoxide in middle conditions. The ^{1}H NMR spectrum of **6** (Figure 1) display several signals at 2.42 ppm for methyl group bound to imidazole ring: at 2.12 ppm for methyl bound to ketone; at 2.66-2.86 ppm for methylene bound to ketone group; at 3.04-3.20 ppm for methylene bound to phenyl group; at 3.62 ppm for methylene group linked to both nitrile and phenyl groups; at 4.88 ppm for methylene bound to ether group; at 6.32 ppm for imidazole ring; at 6.90-7.96 ppm for phenyl groups; at 11.34 ppm for amino group. The ^{13}C NMR spectra showed chemical shifts at 13.92 ppm for methyl group bound to imidazole ring; at 23.44 ppm for methylene group bound to nitrile group; at 30.44 ppm for methyl group linked to ketone group; at 36.84 ppm for methylene group bound to phenyl group; at 49.70 ppm for methylene group bound to ketone group; at 82.30 ppm for methylene group bound to ether group; at 110.62, 141.50 and 151.90 ppm for imidazole ring; at 117.42 ppm for nitrile group; at 11.50-133.66, 147.30 and 153.62-159.32 ppm; at 200.84 ppm for ketone group. In addition, the mass spectrum from **6** showed a molecular ion (m/z) 439.18.

3.1.5. Reduction reaction.

There are several reports on reduction reactions which use some reagents such as TarB-NO2 [21], SmI_2 [22], oxazaborolidine [23], $La[N(SiMe_3)_2]_3$ [24], sodium borohydride [25] and others. In this study, the ketone of compound **5** was reduced in the presence

of sodium borohydride (Figure 3) to form an imidazol-5-naphthalen-pentane-diol derivative (**7**).

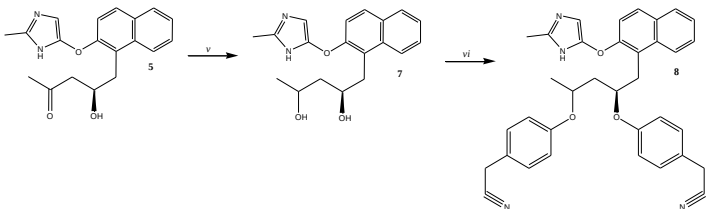

Figure 3. Synthesis of an imidazol-naphthalen-diacetonetrile derivative (**8**). Reaction of a hydroxy-keto derivative (**5**) with sodium borohydride (*v*) to form an imidazol-5-naphthalen-pentane-diol derivative (**7**). Then **7** reacted with 2-(4-nitrophenyl)acetonitrile in the presence of dimethyl sulfoxide (*vi*) to form **8**.

The ^{1}H NMR spectrum of **7** (Figure 1) display several signals at 1.22 ppm for methyl group bound to hydroxyl group: at 1.52-1.56, 2.88 and 4.28 ppm for methylene bound to both hydroxyl and phenyl groups; at 2.42 ppm for methyl group bound to imidazole ring; at 5.70 ppm for both hydroxyl and amino groups; at 6.32 ppm for imidazole ring; at 7.26-7.94 ppm for naphthalene group. The ^{13}C NMR spectra showed chemical shifts at 13.92 ppm for methyl group bound to imidazole ring; at 23.90 ppm for methyl group bound to hydroxyl group; at 37.30-69.82 ppm for methylene groups bound to both hydroxyl and phenyl groups; at 110.62, 141.50 and 191.90 ppm for imidazole ring; at 117.28-133.20, 147.84 and 153.12 ppm for naphthalene group. Additionally, the mass spectrum from **7** showed a molecular ion (m/z) 326.16.

3.1.6. Third etherification.

Finally, compound **7** reacted with 2-(4-nitro-phenyl)acetonitrile in the presence of dimethyl sulfoxide at middle conditions to form el compound imidazol-naphthalen-diacetonetrile derivative (**8**). The ^{1}H NMR spectrum of **8** (Figure 3) display several signals at 1.22 ppm for methyl group involved in the arm linked to both ether and phenyl groups; at 2.02-2.20, 3.00-3.14 and 4.50-5.02 ppm for methylene groups bound to both ether and phenyl groups; at 2.42 ppm for methyl group bound to imidazole ring; at 3.62 ppm for methylene group bound to nitrile group; at 6.32 ppm for imidazole ring; at 6.80-7.92 ppm for phenyl groups; at 11.34 ppm for amino group. The ^{13}C NMR spectra showed chemical shifts at 13.92 ppm for methyl group bound to imidazole ring: at 21.54 ppm methyl group involved in the arm bound to both ether and phenyl groups; at 23.44 ppm for nitrile group; at 36.74-80.27 ppm for methylene groups bound to both ether and phenyl groups; at a110.60, 141.50 and 151.92 ppm for imidazole ring; at 116.08-117.12, 118.34-135.92, 146.56 and 154.44-158.40 ppm for phenyl groups; at 117.40 ppm for nitrile group. Finally, the mass spectrum from **8** showed a molecular ion (m/z) 526.24.

3.2. Pharmacophore ligand model.

Several chemical models have been used to determine the three-dimensional orientation adopted by the functional groups of a molecule to predict its interaction with several biomolecules [26]; for example, the use of a pharmacophore model which can furnish a new insight to design novel molecules that can enhance or inhibit the function of a biological target which can be useful in new drug discovery. Analyzing this premise in this study, the LigandScout software [10, 11] was used to develop a pharmacophore model for compounds **2,3** and **5-8** (Figures 4 and 5). The results showed that functional groups involved in these compounds could interact via hydrophobic contacts or as hydrogen bond acceptors or as hydrogen bond donor with some biomolecules.

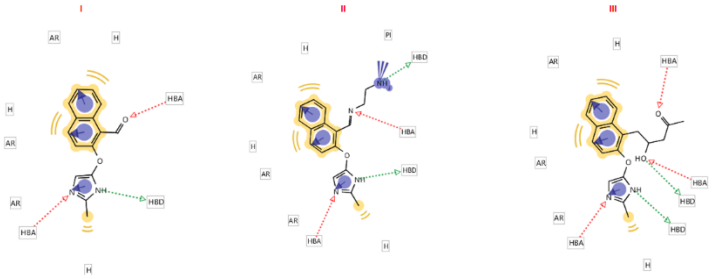

Figure 4. Scheme represents a pharmacophore from either compounds **2**, (I), **3** (II) and **5** (III) using the LigandScout software. The model involves a hydrogen bond acceptors (HBA, red) and hydrogen bond donor (HBD, green).

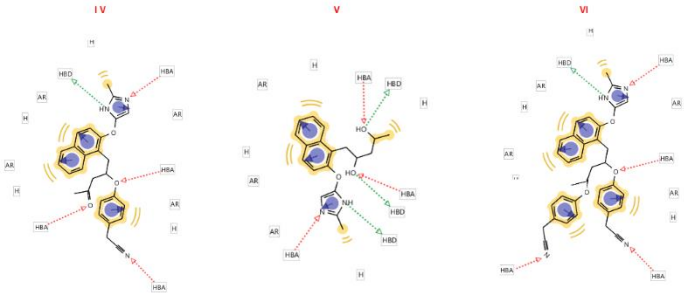

Figure 5. Pharmacophore from either compounds **6**, (IV), **7** (V) and **8** (VI) using the LigandScout software. The model involves a hydrogen bond acceptors (HBA, red) and hydrogen bond donor (HBD, green).

3.3. Interaction theoretical.

There are several studies to predict the interaction of some drugs with protein or enzymes using some theoretical models [27]. This study was carried out a theoretical analysis on interaction of either compounds **2**, **3**, **5-8** with either coronavirus (5epw protein) in a Docking model [13] using both hydroxychloquine and favipiravir as controls. The data (Table 1) showed differences in the interaction of either hydroxychloquine, favipiravir and compounds **2**, **3**, **5-8** with 5ewp protein surface.

Table 1. Aminoacid residues involved between the interaction of compounds 2, 3, 5-8 and hydroxylchloroquine (OHCl-quine), and Favipiravir with 5ewp protein surface.

OHCl-quine	Favipi-ravir	C-2	C-3	C-5	C-6	C-7	C-8
Arg_{238}	Pro_{240}	Arg_{238}	Val_{246}	Pro_{240}	Val_{246}	Pro_{240}	Pro_{240}
Val_{239}	Val_{246}	Val_{239}	Met_{254}	Val_{246}	Phe_{250}	Val_{246}	Val_{246}
Met_{259}	Phe_{250}	Pro_{240}	Leu_{264}	Phe_{250}	Arg_{253}	Met_{259}	Phe_{250}
Leu_{264}	Arg_{253}	Val_{246}	Phe_{274}	Arg_{253}	Met_{259}	Leu_{264}	Arg_{253}
Val_{269}	Met_{259}	Phe_{250}	Leu_{277}	Met_{259}	Leu_{264}	Phe_{274}	His_{257}
Phe_{274}	Leu_{264}	Arg_{253}	Ile_{281}	Leu_{264}	Phe_{274}	Leu_{277}	Asn_{258}
Leu_{277}	Val_{269}	Leu_{264}	Phe_{322}	Phe_{274}	Ile_{281}	Ile_{282}	Leu_{264}
$Ileu_{281}$	Phe_{274}	Val_{269}	Gln_{325}	Leu_{277}	Tyr_{308}	Phe_{322}	Phe_{274}
Gln_{284}		Phe_{274}		Ile_{281}	Phe_{322}	Gln_{325}	Ile_{281}
				Phe_{322}			Gln_{284}

These differences could decrease the biological activity of coronavirus; however, other thermodynamic parameters may be involved in the interaction of these compounds with 5epw protein surface

3.4. Thermodynamic parameters.

To evaluate the hypothesis above mentioned, in this investigation, a theoretical ass was carried out to determinate some thermodynamic factors involved in the interaction of either hydroxychloquine, favipiravir or compounds **2**, **3**, **5-8** with 5ewp protein such as 1) free energy of binding which determinates the

energy value that requires a molecule to interact with a protein in a water environment; 2) electrostatic energy that is the product of electrical charge and electrostatic potential; 3) total intermolecular energy and 4) Van der Waals (vdW) + hydrogen bond (Hbond) + desolvation energy (Desolv. Energy; which have an influence on the movement of water molecules into or out of the ligand-protein [27].

Theoretical results found (Table 2) showed that some differences in the thermodynamic parameters of compounds **2**, **3**, **5-8** compared to either hydroxychloroquine or favipiravir. However, the inhibition constant (Ki) for compounds **3** and **5** was less compared with either hydroxychloroquine, favipiravir and compounds **2**, **6-8**. This phenomenon suggests that compounds **3** and **5** could induce changes in the biological activity of 5ewp protein translated as inhibition of the biological activity of coronavirus.

Table 2. Thermodynamic parameters involve in the interaction of of compounds 2, 3, 5-8 and hydroxylchloroquine (OHCl-quine), and Favipiravir with 5ewp protein surface.

Compound	Est. Fee Energy of Binding (kcal/mol)	Est. Inhi-bition Constant, Ki (μM)	cdW + Hbond + desolv Energy	Electrost. Energy	Total Inter-molec. Energy	Interact. Surface
OHCl-quine	-3.35	7.52	-5.93	0.21	5.72	739.82
Favipiravir	-2.96	6.73	-3.61	0.03	-3.57	365.18
2	-6.55	85.50	-6.31	-0.12	-6.43	569.62
3	-4.02	1.13	-6.23	-0.12	-6.34	658.49
5	-3.81	1.62	-5.75	-0.05	-5.58	625.41
6	-4.48	520.24	-7.82	0.03	-7.79	944.44
7	-4.68	368.55	-6.60	0.04	-6.57	659.65
8	-4.52	482.99	-9.18	-0.07	-9.24	1062.51

4. CONCLUSIONS

In this study, the facile synthesis of some imidazole derivatives using several chemical strategies is reported. In addition, Theoretical analysis of the interaction between compound imidazole derivatives, showed a higher affinity of compounds **3** and **5** by the 5ewp protein which is translated as a possible inhibition of biological activity of coronavirus.

5. REFERENCES

1. Clark, R.; Millar, J.; Baillie, K. Clinical evidence does not support corticosteroid treatment for 2019-nCoV lung injury. *The Lancet* **2020**, *395*, 473-475, https://doi.org/10.1016/S0140-6736(20)30317-2.
2. Liu, J.; Liao, X.; Qian, S.; Yuan, J.; Wang, F.; Liu, Y.; Zhang, Z. Community Transmission of Severe Acute Respiratory Syndrome Coronavirus 2, Shenzhen, China, 2020. *Emerging infectious diseases* **2020**, *26*, https://doi.org/10.3201/eid2606.200239.
3. Backer, J.; Klinkenberg, D.; Wallinga, J. Incubation period of 2019 novel coronavirus (2019-nCoV) infections among travellers from Wuhan, China. *Eurosurveillance* **2020**, *25*, 20-28, https://doi.org/10.2807/1560-7917.ES.2020.25.5.2000062.
4. Zhang, H.; Zhang, H.; Kemnitzer, W.; Tseng, B.; Cinatl, J.; Michaelis, M.; Cai, S. Design and synthesis of dipeptidyl glutaminyl fluoromethyl ketones as potent severe acute respiratory syndrome coronovirus (SARS-CoV) inhibitors. *Journal of Medicinal Chemistry* **2006**, *49*, 1198-1201. https://doi.org/10.1021/jm0507678
5. Zhang, L.; Lin, D.; Kusov, Y.; Nian, Y.; Ma, Q.; Wang, J.; De-Wilde, A. α-Ketoamides as broad-spectrum inhibitors of coronavirus and enterovirus replication: Structure-based design, synthesis, and activity assessment. *Journal of Medicinal Chemistry* **2020**, https://doi.org/10.1021/acs.jmedchem.9b01828.
6. Zhou, L.; Liu, Y.; Zhang, W.; Wei, P.; Huang, C.; Pei, J.; Lai, L. Isatin compounds as noncovalent SARS coronavirus 3C-like protease inhibitors. *Journal of Medicinal Chemistry* **2006**, *49*, 3440-3443, https://doi.org/10.1021/jm0602357.
7. Jacobs, J.; Grum-Tokars, V.; Zhou, Y.; Turlington, M.; Saldanha, S.; Chase, P.; Mielech, A. Discovery, synthesis, and structure-based optimization of a series of N-(tert-butyl)-2-(N-arylamido)-2-(pyridin-3-yl) acetamides (ML188) as potent noncovalent small molecule inhibitors of the severe acute respiratory syndrome coronavirus (SARS-CoV) 3CL protease. *Journal of Medicinal Chemistry* **2013**, *56*, 534-546, https://doi.org/10.1021/jm301580n.
8. Ghosh, A.; Takayama, J.; Rao, K.; Ratia, K.; Chaudhuri, R.; Mulhearn, D.; Johnson, M. Severe acute respiratory syndrome coronavirus papain-like novel protease inhibitors: design, synthesis, protein− ligand X-ray structure and biological evaluation. *Journal of Medicinal Chemistry* **2010**, *53*, 4968-4979, https://doi.org/10.1021/jm1004489.
9. Zhang, J.; Pettersson, H.; Huitema, C.; Niu, C.; Yin, J.; James, M.; Vederas, J. Design, synthesis, and evaluation of inhibitors for severe acute respiratory syndrome 3C-like protease based on phthalhydrazide ketones or heteroaromatic esters. *Journal of Medicinal Chemistry* **2007**, *50*, 1850-1864, https://doi.org/10.1021/jm061425k.
10. Saxena, S.; Abdullah, M.; Sriram, D.; Guruprasad, L. Discovery of novel inhibitors of Mycobacterium tuberculosis MurG: Homology modelling, structure-based pharmacophore, molecular docking, and molecular dynamics simulations. *Journal of Biomolecular Structure and Dynamics* **2018**, *36*, 3184-3198, https://doi.org/10.1080/07391102.2017.1384398.
11. Kainrad, T.; Hunold, S.; Seidel, T.; Langer, T. LigandScout Remote: A new User-Friendly Interface for HPC and Cloud Resources. *Journal of Chemical Information and Modeling* **2018**, *59*, 31-37, https://doi.org/10.1021/acs.jcim.8b00716.
12. Abdul-Rasool, S.; Fielding, B. Understanding human coronavirus HCoV-NL63. *The Open Virology Journal* **2010**, *4*, 76.
13. Saxena, S.; Abdullah, M.; Sriram, D.; Guruprasad, L. Discovery of novel inhibitors of Mycobacterium tuberculosis MurG: Homology modelling, structure-based pharmacophore, molecular docking, and molecular dynamics simulations. *Journal of Biomolecular Structure and Dynamics* **2018**, *36*, 3184-3198, https://doi.org/10.1080/07391102.2017.1384398.
14. Nishimoto, Y.; Kang, K.; Yasuda, M. Regio-and Stereoselective Anti-Carbozincation of Alkynyl Ethers Using ZnBr2 toward (Z)-β-Zincated Enol Ether Synthesis. *Organic Letters* **2017**, *19*, 3927-3930, https://doi.org/10.1021/acs.orglett.7b01847.
15. Chen, X.; Xiao, X.; Sun, H.; Li, Y.; Cao, H.; Zhang, X.; Lian, Z. Transition-Metal-Catalyzed Transformation of Sulfonates via S–O Bond Cleavage: Synthesis of Alkyl Aryl Ether and Diaryl Ether. *Organic Letters* **2019**, *21*, 8879-8883, https://doi.org/10.1021/acs.orglett.9b02858.

16. Kuriyama, M.; Matsuo, S.; Shinozawa, M.; Onomura, O. Ether-Imidazolium Carbenes for Suzuki–Miyaura Cross-Coupling of Heteroaryl Chlorides with Aryl/Heteroarylboron Reagents. *Organic Letters* **2013**, *15*, 2716-2719, https://doi.org/10.1021/ol4010189.
17. Nakajima, M.; Orito, Y.; Ishizuka, T.; Hashimoto, S. Enantioselective aldol reaction of trimethoxysilyl enol ether catalyzed by lithium binaphtholate. *Organic Letters* **2004,** *6*, 3763-3765, https://doi.org/10.1021/ol048485+.
18. Figueroa-Valverde, L.; Diaz-Cedillo, F.; García-Cervera, E.; Gómez, E.; Rosas-Nexticapa, M.; López-Ramos, M.; May-Gil, I. Design and Synthesis of an Aromatic-steroid Derivative. *Oriental Journal of Chemistry* **2013**, *29*, 465-468.
19. Yamada, Y.; Yoshikawa, N.; Sasai, H.; Shibasaki, M. Direct catalytic asymmetric aldol reactions of aldehydes with unmodified ketones. *Angewandte Chemie International* **1997**, *36*, 1871-1873, https://doi.org/10.1002/anie.199718711.
20. List, B.; Pojarliev, P.; Castello, C. Proline-catalyzed asymmetric aldol reactions between ketones and α-unsubstituted aldehydes. *Organic Letters* **2001**, *3*, 573-575, https://doi.org/10.1021/ol006976v.
21. Eagon, S.; DeLieto, C.; McDonald, W.; Haddenham, D.; Saavedra, J.; Kim, J.; Singaram, B. Mild and Expedient Asymmetric Reductions of α, β-Unsaturated Alkenyl and Alkynyl Ketones by TarB-NO2 and Mechanistic Investigations of Ketone Reduction. *The Journal of organic chemistry* **2010**, *75*, 7717-7725, https://doi.org/10.1021/jo101530f.
22. Chciuk, T.; Anderson, W.; Flowers, R. Reversibility of Ketone Reduction by SmI2-Water and Formation of Organosamarium Intermediates. *Organometallics* **2017**, *36*, 4579-4583, https://doi.org/10.1021/acs.organomet.7b00392.
23. Xu, J.; Wei, T.; Zhang, Q. Effect of temperature on the enantioselectivity in the oxazaborolidine-catalyzed asymmetric reduction of ketones. Noncatalytic borane reduction, a nonneglectable factor in the reduction system. *The Journal of organic chemistry* **2003**, *68*, 10146-10151, https://doi.org/10.1021/jo035203v.
24. Weidner, V.; Barger, C.; Delferro, M.; Lohr, T.; Marks, T. Rapid, mild, and selective ketone and aldehyde hydroboration/reduction mediated by a simple lanthanide catalyst. *ACS Catalysis* **2017** *7*, 1244-1247, https://doi.org/10.1021/acscatal.6b03332.
25. Nguyen, T.; Huang, C.; Doong, R. Enhanced catalytic reduction of nitrophenols by sodium borohydride over highly recyclable Au@ graphitic carbon nitride nanocomposites. *Applied Catalysis B: Environmental* **2019**, *240*, 337-347, https://doi.org/10.1016/j.apcatb.2018.08.035.
26. Sciortino, G.; Rodríguez P.; Lledós, A.; Garribba, E.; Maréchal, J. Prediction of the interaction of metallic moieties with proteins: An update for protein-ligand docking techniques. *Journal of Computational Chemistry* **2018**, *39*, 42-51, https://doi.org/10.1002/jcc.25080.
27. Figueroa L.; Diaz, F.; Rosas, M.; Mateu, V. Design and synthesis of two steroid derivatives from 2-nitroestrone and theoretical evaluation of their interaction with BRCA-1. *Asian Journal of Green Chemistry*. **2019**, *3*, 216-235, https://dx.doi.org/10.22034/ajgc.2018.144189.1093.

6. ACKNOWLEDGEMENTS

To Benjamin Valverde and Raquel Anzurez, for your unconditional support on this manuscript.